

ENHANCED VISIBLE RADIANCE NEAR CLOUDS IN THE OCTS MEASUREMENTS

T. Kobayashi, K. Masuda, and A. Uichiyama

Meteorological Research Institute, Japan

Received December 7, 1998

Accepted January 18, 1999

Enhanced visible radiance was found in clear-air fields of view near a broken cloud, in the OCTS measurements. No meaningful change in the corresponding brightness temperature was observed, so the enhanced radiance is thought to be due to the effects of clouds near the fields of view (FOV). If a broken cloud exists in the vicinity of the FOV, the solar radiation reflected from the solar side of the cloud enters the FOV and may enhance the measured radiance. An increase of about 5% in the radiance near clouds was measured by comparing it with the radiance in a region 10 km from the cloud at a wavelength of 0.412 μm . The enhanced radiance measured by the OCTS sensor almost coincides with the Monte Carlo simulation.

1. INTRODUCTION

The Ocean Color and Temperature Scanner² (OCTS) is one of eight sensors equipped on the Advanced Earth Observing Satellite (ADEOS) which was launched in August 1996. The OCTS sensor is similar to the Coastal Zone Color Scanner (CZCS) and is designed to provide enough sensitivity for retrieving the ocean primary production and the sea surface temperature. Unfortunately, the ADEOS stopped taking measurements in the summer 1997, but useful data had been obtained by then.

In using space-borne sensors to derive surface properties, accurate atmospheric correction is needed because of the significant contributions of atmospheric scattering. One of the important issues to improve the algorithm for atmospheric correction is the inclusion of the effects of multiple scattering and the effects of horizontally inhomogeneous ground surfaces and atmospheres. If there are bright land areas adjacent to the dark target pixel, as in coastal areas, a higher reflection from the land areas enhances the radiance received at a satellite sensor and therefore leads to a bias in the retrieved surface reflectivity, which is known as the adjacency effect.

Similarly, horizontally inhomogeneous atmospheres, which often appear in cloudy conditions, also affect the signals detected at a satellite sensor. Even if fields of view (FOV) are homogeneous and cloud-free, a broken cloud near the FOV influences the atmospheric scattering through in-FOV and out-FOV radiative interaction. Some photons from the sun, atmosphere and the ground surface, scattered by clouds enter into the satellite field of view and consequently enhance the radiance detected at a satellite-borne sensor. This enhanced radiation leads to a bias in the derived surface reflectivity and atmospheric properties

if 1-D radiative transfer models, as is commonly done, are applied for atmospheric correction (Ref. 4). Hereafter, we refer to this cloud as the adjacent cloud and to this effect as the cloud adjacency effect. The purpose of the present study is to examine the effect of the adjacent cloud from the OCTS measurements. Note that we focus on the enhanced radiance and ignore the effects of shadowing or obscuring by clouds.

2. OCTS MEASUREMENTS

Radiance received at a space-borne sensor (L) for the surface-atmosphere system is given by

$$L = L_{\text{pa}} + L_{\text{r}} + L_{\text{n}},$$

where, L_{pa} denotes the atmospheric scattering contribution that is caused by radiation scattered in the atmosphere without the surface reflection and is called the atmospheric path radiance,¹ L_{r} is the surface reflection contribution, and L_{n} is the surface-atmosphere interaction term. In deriving surface properties from space, the atmospheric scattering contribution should be removed from the measured radiance. If a cloud is located near the FOV in which a cloud-free field is assumed, some photons scattered by the adjacent cloud enter the FOV and enhance the path radiance. This enhanced radiance is thought to occur in regions very near the clouds. Therefore, a sensor with a high spatial resolution is needed to examine the cloud adjacency effect.

The OCTS had an excellent spatial resolution (700 m at nadir) and therefore can be applied to examine the cloud adjacency effect. An enhanced radiance near a cloud may be detected. However, enhanced radiance occurs in situations other than the cloud adjacency effect, such as optically thicker atmospheres, like thin clouds near the FOV. We have

to distinguish this effect from the cloud adjacency effect. Fortunately, the ADEOS has three infrared sensors as well as visible channels. Over a warm sea surface, a much lower brightness temperature will be expected for a cloud pixel, which can easily be distinguished from a clear region, and because no cloud adjacency effect appears for infrared radiance, we can identify the cloud adjacency effect by use of the infrared measurements.

Figure 1 shows an image measured with the OCTS at a wavelength of $0.412 \mu\text{m}$ over the North-East Pacific ocean near Japan, on 26 April 1997. White areas are clouds. The right side of a cloud in the center of Fig. 1 was illuminated by the sun. The solar zenith angle was about 23° and the azimuth angle was about 143° from the north. Homogeneous clear areas are extended in the right side of the cloud but thin clouds appear in the left side.

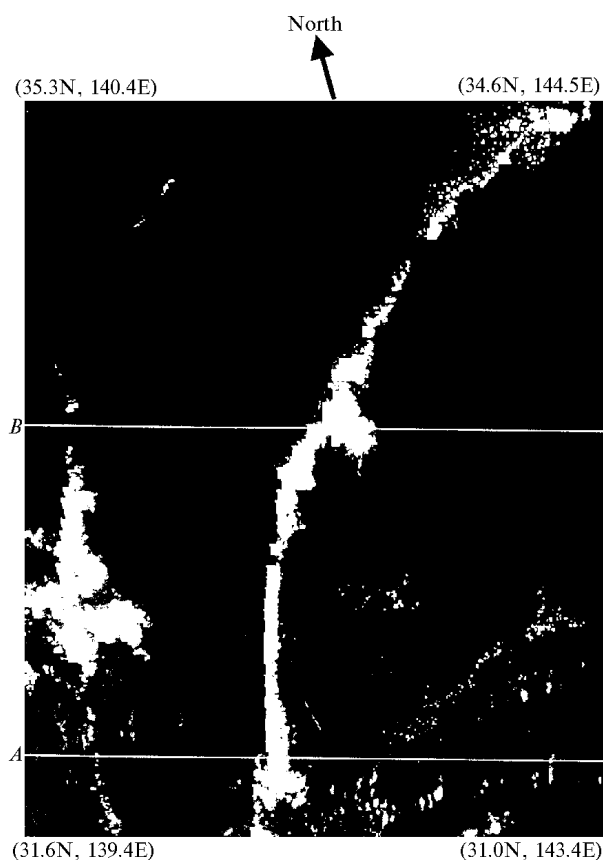


FIG. 1. OCTS image measured over the North-East Pacific ocean in April 1997.

Figure 2 shows a cross section of the measured radiances along the line A in the right side of the cloud indicated in Fig. 1 at three visible wavelengths 0.412 , 0.490 , and $0.565 \mu\text{m}$, and the brightness temperature at a wavelength of $12.0 \mu\text{m}$ near the cloud. One pixel of the OCTS sensor corresponds to about 700 m . The region of higher reflection at the visible wavelengths and lower brightness temperature is a cloud. The vertical dash-space line indicates the boundary of the clear-air and the cloud regions. Almost constant values of the small visible radiance and high brightness

temperature appear in regions about 10 km apart from the clear-air boundary (pixel number exceeding 255) which suggests that homogeneous clear atmospheres are in this region. The visible radiance and the brightness temperature of the clear atmosphere are indicated by dashed lines. In the clear-air region very near the clear-air boundary, a slight increase in the visible radiances is observed. The fact that there is a slight decrease in the brightness temperature in the same area suggests that there is a thin cloud or thick aerosols in this area. A thin cloud is probably the reason for the increased radiance because of the weak spectral dependence of the increase in the visible radiance.

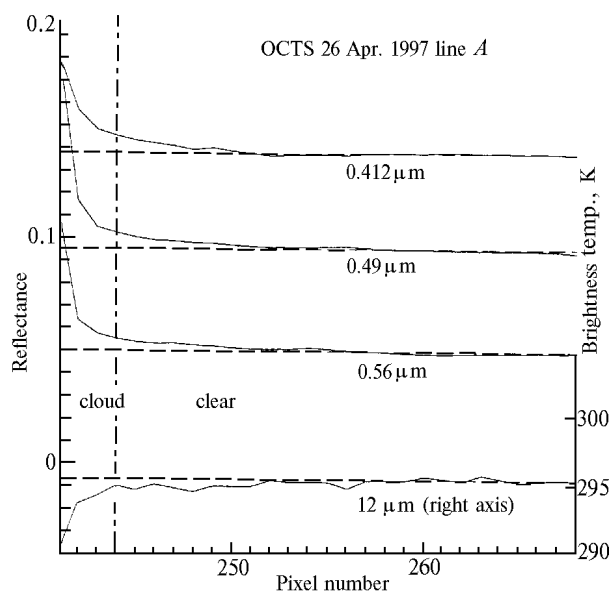


FIG. 2. Cross section of the OCTS radiance along the line A indicated in Fig. 1.

Figure 3 is the same as Fig. 2 but along the line B in the right side of the cloud indicated in Fig. 1. The sharp increase (decrease) in the visible radiance (brightness temperature) suggests that the cloud has a distinct boundary. Almost constant values of the visible radiance and brightness temperature appear about 10 km distance from the clear-air boundary (pixel number exceeding 330), and a slight increase in the visible radiance is observed in the clear-air region very near the boundary, as in Fig. 2. For the brightness temperature, however, no apparent change is observed in this region, so that neither cloud nor thick aerosols are thought to exist near the boundary. The radiance at a wavelength of $0.412 \mu\text{m}$ near the boundary increases by about 5% compared with the radiance in a region 10 km from the clear-air boundary.

The 5% increase in the visible radiance, however, could also occur from a slight increase in the aerosol concentrations. Rayleigh and aerosol optical thicknesses in the clear-air region are estimated as about 0.15 and 0.2 , respectively, at a wavelength of $0.49 \mu\text{m}$. Clear-air reflected radiance is almost linearly related to the optical thickness, so that a slight increase in the aerosol

optical thickness by 0.018 leads to an increased visible radiance of 5% but may not affect the brightness temperature. Therefore, we cannot distinguish the cloud adjacency effect from this aerosol effect. However, the decreasing tendency of the measured enhanced radiance with the increasing distance from the boundary is very similar to the theoretical calculations as shown in the next section. The increase in the visible radiance near the boundary shown in Fig. 3 is, therefore, thought to be due to the cloud adjacency effect. In the next section we will examine the OCTS measurements by comparing them with Monte Carlo simulations.

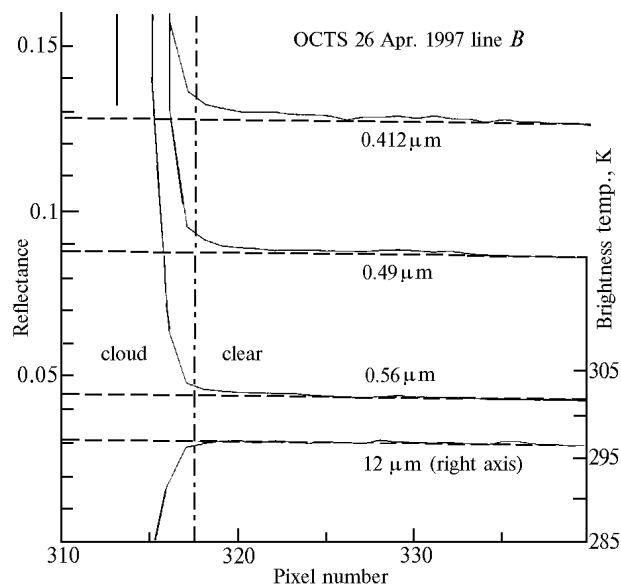


FIG. 3. Same as Fig. 2 but along the line B in Fig. 1.

3. MONTE CARLO SIMULATIONS

In order to examine the enhanced radiance measured with the OCTS, we performed Monte Carlo simulations. The Monte Carlo model used in this study is similar version by Kobayashi et al.³ Photon trajectories are calculated in a conventional manner. The distance that the photon travels until it interacts with a particle and the scattering angle are determined by the volume scattering coefficient and the phase function. The radiance detected by a satellite sensor is, however, calculated stochastically to improve the computational efficiency (Ref. 5).

The geometry of the cloud is assumed to be an infinitely-long cuboidal bar to simulate the measured line-shaped cloud shown in Fig. 1. The height of the cloud top is assumed to be 4 km, which is estimated from the measured brightness temperature at the cloud top of 2°C and the sea surface temperature of 25°C. We have no available information to estimate the cloud bottom height, so we assumed the height to be 2 km. The cloud width is assumed to be 2 km. The cloud extinction coefficient is taken to be 5 km⁻¹. The phase function was calculated by assuming a log-normal function for the droplet size distribution of the water

clouds. The standard deviation is taken to be 1.41 μm, and the median radius is taken to be 2.94 μm. The refractive index of cloud droplets is assumed to be 1.335. The vertical profiles of the molecules and the aerosol particles density are assumed to be the Mid-latitude Summer model tabulated by McClatchey et al.⁶ The size distribution of aerosols particles is also assumed to be described by a log-normal function (oceanic aerosols model⁷), but the standard deviation and the median radius are taken to be 2.51 μm and 0.30 μm, respectively.

The spatial resolution of the sensor is taken to be 2 km×2 km at nadir. The satellite sensor is specified to look in the nadir direction. The solar zenith angle is 25° and the azimuth angle is 135° with respect to the north. For the present computations, the number of trials was set at 30,000,000.

Figure 4 shows the Monte Carlo results and the OCTS measurements along line B indicated in Fig. 1.

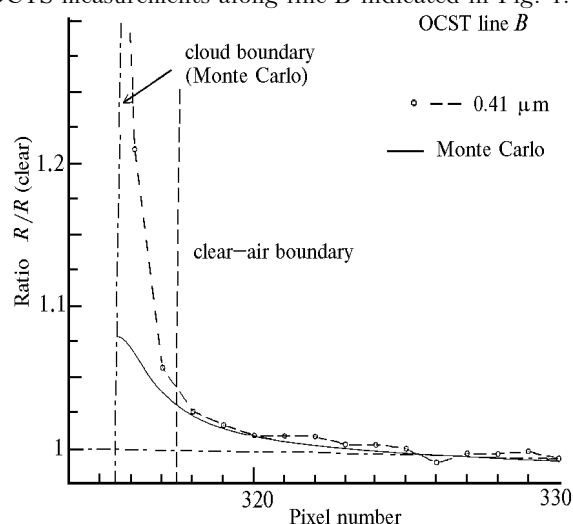


FIG. 4. Comparisons of the Monte Carlo results and the OCTS measurements at a wavelength of 0.412 μm. A ratio of the radiance to that at the clear-air region 10 km from the clear-air boundary is plotted.

The radiances divided by the clear-air radiances at 10 km from the clear-air boundary are plotted at a wavelength of 0.412 μm. The cloud boundary for the Monte Carlo simulations is assumed to be the pixel number of 315.5 at which a significant increase in the radiance is observed. The Monte Carlo results almost agree with the OCTS measurements in the clear-air region near the boundary. The simulation condition applied to the Monte Carlo model may not be coincident with the measurements, like the surface albedo = 0. This difference may not lead to the decreasing tendency of the ratio with the distance.

4. DISCUSSIONS AND CONCLUSIONS

Enhanced visible radiance was found in clear-air fields of view near broken clouds in the OCTS measurements. If a broken cloud exists in the vicinity of the FOV, the solar radiation reflected from the solar

side of the cloud enter the FOV and may enhance the measured radiance. However, the radiance enhancement could also occur from observational errors and thin clouds near the cloud boundary. Because a space-borne sensor has finite time memory, the radiance of a dark clear area will be affected by a bright cloud area if the sensor is scanning from the bright area to the dark area. The enhancement due to this observational error will have small wavelength dependence. However, the enhanced radiation at a wavelength of $0.565\ \mu\text{m}$ is much smaller than that at $0.412\ \mu\text{m}$ (Fig. 3) which suggests that the measured enhanced radiance did not arise from the observational error. Thin clouds may affect infrared radiance to some degree (Fig. 2). However, no meaningful change in the corresponding brightness temperature was observed in Fig. 3. Therefore, the enhanced radiances shown in Fig. 3 are thought to be due to the cloud adjacency effect.

An increase of about 5% in the radiance near clouds at a wavelength of $0.412\ \mu\text{m}$ was measured by comparing it with the radiance in a region 10 km from the clouds. The enhanced radiance measured by the OCTS sensor almost coincides with the Monte Carlo simulation. There is still possibility that increased aerosols concentrations near clouds introduce the enhanced radiance which is difficult to be identified. Polarization measurements which was also made on the ADEOS satellite (POLDER: Polarization and Directionality of the Earth's

Reflectances) may be useful to distinguish the cloud adjacency effect from a small spatial change in the aerosol concentrations.

ACKNOWLEDGMENT

A part of the present study was supported by the National Space Development Agency of Japan.

REFERENCES

1. J.F.W. de Haan, Hovenier, J.M.M. Kokke, and H.T.C. van Stokkom, *Remote Sens. Environ.* **37**, 1–21 (1991).
2. H. Kawamura et al., *J. Oceanogr.* **54**, 383–399 (1998).
3. T. Kobayashi, *J. Atmos. Sci.* **45**, 3034–3045 (1988).
4. T. Kobayashi, K. Masuda, and M. Sasaki, *Enhanced visible radiance in clear-air fields of view adjacent to clouds: Monte Carlo simulations* (in preparation).
5. K.E. Kunkel and J.A. Weinman, *J. Atmos. Sci.* **33**, 1712–1781 (1976).
6. R.A. McClatchey, R.W. Fenn, J.E.A. Selby, F.E. Volz, and J.S. Garing, *Optical properties of the atmosphere*, AFCRL-72-0497 (1972).
7. E.P. Shettle and R.W. Fenn, *Models of the atmospheric aerosols and their optical properties*, AFGARD-CP-183 (1976).